TRUE OR NOT TRUE: CARBON-FREE ELECTRICITY GENERATION IS POSSIBLE

Simen Gaure and Rolf Golombek

Working Paper 11/2019

CREE – Oslo Centre for Research on Environmentally Friendly Energy
acknowledges financial support from
The Research Council of Norway, University of Oslo and user partners.
ISBN: 978-82-7988-279-4
ISSN: 1892-9680
http://www.cree.uio.no

Abstract in Norwegian:

CREE - Working Paper 11/2019

Er det mulig med en karbonfri europeisk elektrisitetssektor?

Simen Gaure and Rolf Golombek

For å oppnå en samlet utslippsreduksjon i drivhusgasser på minst 80 prosent innen 2050, sikter EU mot å redusere utslippene i kraftsektoren med 95 prosent. Ved bruk av detaljerte værdata med timesoppløsning for perioden 2005-16 viser vi at EU kan designe en kraftsektor der vind og solkraft har en markedsandel på 98 prosent. Dette krever imidlertid omfattende lagring av elektrisitet; i den mest krevende timen må en energimengde som svarer til 5 prosent av årskonsumet av elektrisitet i Europa, lagres.

TRUE OR NOT TRUE:

CARBON-FREE ELECTRICITY GENERATION IS POSSIBLE[1]

Simen Gaure and Rolf Golombek

Frisch Centre

December 10, 2019

ABSTRACT

A key component in the transition to a low-emission society is radical emissions reductions in the electricity generation sector. The EU, for example, aims at reducing emissions from electricity plants by 95 percent as part of their goal of lowering total GHG emissions by at least 80 percent by 2050. Using re-analysis data for the period 2005-16 and simulations, we show how the EU can design an electricity generation sector where around 98 percent of total production is generated by wind power and solar. In our reference case, a large amount of batteries must be installed to make the system work. In the most demand hour in the period 2006-15, an amount of electricity corresponding to 5 percent of average annual consumption of electricity has to be stored in the batteries. Average annual use of batteries corresponds to 15 percent of average annual consumption of electricity.

[1] Both authors are associated with CREE - the Oslo Centre for Research on Environmentally friendly Energy, which is supported by the Research Council of Norway. Earlier versions of this paper have been presented at the Bergen Economics of Energy and Environment Research Conference, Oslo Energy Transitions Workshop, the Norwegian Ministry of Petroleum and Energy, the Norwegian Water Resources and Energy Directorate and Statkraft – we thank the participants for their comments. This research was made possible through financial support from the Research Council of Norway to the CREE centre.

Introduction

Signatories to the Paris Agreement aim to keep the rise in global average temperature well below 2 degrees Celsius above pre-industrial levels. A key component in the transition to a low-emission society is a radical emissions reduction in the electricity generation sector. The EU, for example, aims at reducing emissions from electricity plants by 95 percent as part of their goal of lowering total GHG emissions by at least 80 percent by 2050. This paper examines how the EU can reach the emissions target for the electricity generation sector.

Which electricity technologies are available to meet the EU policy goal of a 95 percent emissions reduction? Obviously, conventional fossil-fuel technologies have to be phased out as these generate the problem. Conventional fossil-fuel based technologies coupled with *C*arbon *C*apture and *S*torage (CCS) might have a potential, but de facto no European country plan to invest in these technologies due to, for example, high costs or extensive resistance to store carbon below the ground. Nuclear, which has a substantial market share in Europe (around 25 percent), will hardly be expanded; some countries plan to phase out nuclear, whereas others may replace existing capacity with new capacity – overall nuclear capacity in the EU might decrease over time. There is a potential for expansion of hydroelectricity (in 2015 its market share was around 10 percent), but national plans clearly suggest limited potential. Also bio power has a potential for expansion, but the increase may be moderate because land used for growing inputs to bio electricity has alternative use. In addition, the standard assumption that bio power is carbon free has clearly been questioned, see, for example, Searchinger et al. (2017). Hence, in the future electricity production in the EU must mainly come from other technologies, which means wind power and solar.

A key characteristic of wind and solar power is intermittency; the level of production cannot be controlled; it is determined by installed capacity and the weather conditions (wind speed or solar irradiance). This is in stark contrast to fuel-based power plants. Due to the intermittency of wind and solar, there will in general be a mismatch between production from these sources and consumption. Intermittent production will fluctuate much more than consumption, and the "average" daily path of production may also differ from the standard consumption profile over the day. Therefore, it might be socially desirable to link production from intermittent power stations to a storage technology, thereby ensuring that production in each point in time matches the load.

The purpose of the present study is to examine whether it is possible to design an electricity generation sector in Europe that is carbon free. To make the problem as tough as possible, in most of the discussion we neglect existing electricity capacities; some of these, in particular, reservoir hydro and nuclear, will make the EU goal of a 95 percent emissions reduction easier to accomplish. In Section 5, we discuss, however, how non-intermittent technologies may be helpful in achieving the EU emission target. Thus, below we mainly study the design of an electricity generation sector consisting of wind power, solar power and a storage technology, here batteries, for Europe. However, if necessary for making the system work, we allow for investment in a back-up technology that can rapidly change its production over the day.

There is a growing literature on whether it is possible to transform the electricity sector, and even the whole energy system, into one without any, or only tiny, emissions. Some examples are Breyer et al. (2017), Elliston et al. (2012), Elliston et al. (2014), Koskinen and Breyer (2016), Mai et al. (2014), Rasmussen et al. (2012), Salomon et al. (2018) and Sgouridis et al. (2016).

Using hourly data for 2014, Sinn (2017) studies the limits of Germany's energy revolution, that is, to phase out nuclear and fossil-fuel based electricity, allowing for investment in wind power, solar power, hydroelectricity, and international grid expansion as well as demand management. With trade and investment in five European countries, the aggregate electricity market share of wind and solar in these countries is around 50 percent. In contrast to Sinn, we allow for investment in batteries, but in our reference case there is only one back-up technology in addition to wind power and solar. Moreover, we study 23 European countries without trade as well as a fully integrated European electricity market. For the latter case, the market share of wind and solar is 98 percent. This solution requires, however, massive investment in batteries: average annual use of batteries corresponds to 15 percent of average annual consumption of electricity in these 23 countries.

Jacobsen et al. (2015) argues that it is possible to electrify all US energy sectors without any use of natural gas, biofuels, nuclear power and stationary batteries. The resulting social cost of a 2050-55 US energy system based entirely on wind, water and solar, is, according to this study, lower than the cost of a fossil-fuel based system. A key characteristic of the proposed energy system is storage of heat in soil and extensive use of hydroelectricity and hydrogen.

Clack et al. (2017) dispute the main finding in Jacobsen et al. (2015), namely that it is possible to design a US energy system based entirely on electricity and hydrogen as energy carriers.

They argue that the Jacobsen et al. study has significant short-comings, for example, invalid modeling tools, modeling errors and that it relies on implausible assumptions. They advise policy makers to treat studies proposing energy systems that relies almost exclusively on wind, solar and hydroelectricity with much caution.

In contrast to Jacobsen et al. (2015), who uses a 3D climate/weather model to predict wind and solar output (for the US for the period 2050-55), we simulate the dispatch from wind and solar power using re-analysis data for the observed period 2006-15 with hourly resolution. Our analysis is restricted to the electricity sector, whereas the Jacobson study covers the entire energy system. Both studies restrict attention to wind, water and solar technologies, but the Jacobson study has a wider portfolio of technologies; we mainly focus on onshore wind, offshore wind and solar, but also discuss the role of reservoir hydro in the concluding remarks. Like Jacobson et al. (2015), we conclude that a wind-water-solar based system is feasible, but in contrast to the Jacobson study, this is not a low-cost system due to heavy investment in batteries.

2 Data

To simulate production from wind and solar, we need data on weather conditions. Instead of estimating how the future weather will turn out, we use data on observed weather to simulate the dispatch from wind and solar power.

From MERRA-2 (The Modern-Era Retrospective analysis for Research and Applications, version 2), see Gelaro et. al (2017), we have access to hourly weather observations for the period 2006-2015 for each of 23 European countries, with a latitude-longitude grid of cells of $0.5° \times 0.625°$. Roughly, each cell is 50 km by 50 km of size. The region for offshore wind power is defined as 12 nautical miles from the coastal line of a country (contiguous zone). In total, we have 2703 (onshore and offshore) cells.

Because wind and sun conditions differ between cells within a country, we mainly focus on the 10 percent best cells within each country; this rule is applied for *each* of the three renewable electricity technologies covered in the present study; onshore wind, offshore wind, and solar. It seems reasonable that development of renewable electricity mainly will take place in these areas.

Wind speed data is used to estimate wind power production 100 meter above the ground, both for onshore and offshore wind power. We use standard assumptions about the power curve – the relationship between wind speed and wind energy: below a cut off (3.5 m/s), wind speed is too low to generate wind power. Above this cut off, there is a steep (cubic) relationship between wind speed and wind energy, but this relationship levels off as wind speed approaches 14 m/s. If wind speed is even higher, there will be no change in wind energy, but above 25 m/s, the wind mill will stop production in order to avoid technical damages.

We use Merra-2 data for wind speed at 50 meter above the ground, and the surface roughness coefficient, to estimate wind speed 100 meter above the ground, see Ruedas et al. (2011) for the methodology. Generated wind energy depends on wind speed 100 meter above the ground, the power curve and the Merra-2 variable air density, see the Appendix for documentation. If wind conditions are optimal in the course of one hour, that is, if wind speed is always between 14 and 25 m/s, 1 MW installed wind power capacity will generate 1 MWh wind energy. We use the same power curve for onshore wind and offshore wind.

Surface incoming shortwave ground flux (SWGDN) data is used to estimate solar power production. We distinguish between direct and indirect radiation to tilted solar panels, and take albedo (diffuse reflection) also into account. Whereas Merra-2 had detailed information on direct radiation and albedo, we had to estimate diffuse radiation, see the Appendix. As part of the calculations, we find optimal (fixed) tilting across the high resolution grid in each of the 23 European countries for solar farms. If solar conditions are optimal, that is, if solar radiation is measured at noon on vernal equinox or autumnal equinox, at equator, and there are no clouds, then 1 MW solar capacity will, in the course of one hour, generate 1 MWh solar energy.

Because we are interested in the mismatch between intermittent production and consumption, we need data also for the load. From ENTSO-E and NORDPOOL we have hourly data on national consumption for each of 23 European countries for the period 2006-15.

3 Simulations

Because the production path of intermittent electricity will never match the load profile, we want to design the electricity generation system so that the mismatch is minimized. Let y_t^i be production (in a country) from technology i, $i =$ offshore wind power, onshore wind power, solar, in period t. Production depends on this technology's share (α^i) of total intermittent

capacity (K), as well as the productivity of this technology in period *t*, β_t^i (measured in MWh per MW installed capacity), where $0 \le \beta_t^i \le 1$. Hence, $y_t = \beta_t^i \alpha^i K$ where $\sum_i \alpha^i = 1$. Because we consider wind and solar power in the 10 percent best cells of each technology (in a country), and we assume that total capacity of a technology ($\alpha^i K$) is distributed evenly between these 10 percent best cells, β_t^i reflects average productivity of the 10 percent best cells of technology *i* in time period *t* (in a country).

Let x_t be consumption of electricity in period *t* (in a country), and let $z_t = \sum_i y_t^i - x_t$, that is, the difference between total production of intermittent electricity and consumption, henceforth referred to as excess electricity in period *t*. Our concern for the mismatch between production and consumption of electricity suggests to choose total intermittent capacity (K) and technology shares (α^i) so as to minimize the (hourly) variance of excess electricity over the period 2006-15. To make the problem interesting, we have to impose a restriction on how much electricity to produce. In our reference case, we impose that for the period 2006-15, total production from the three renewable technologies has to be equal to (observed) total consumption (in a country). We solve the constrained minimization problem for each of the 23 European countries, as well as for a constructed "country" that covers the area of these 23 countries, henceforth referred to as EU-23.FB (*F*irst *B*est). Also for EU-23.FB, we consider the 10 percent best cells for each technology.

The optimal technology shares are shown in Figure 1. For most countries, the technology share of solar is around 40 percent. For countries with a coast line, the technology share of offshore wind power varies between 15 percent and 60 percent. The bar termed EU-23.m shows the unweighted average (*M*ean) of the technology shares of the 23 countries. As seen from the Figure, the technology shares for solar, onshore wind and offshore wind is around 40 percent, 40 percent and 20 percent, respectively.

Once we have derived the optimal technology shares and total renewable capacity of a country, we can use the weather data to simulate production from each technology, and thus calculate excess electricity production in each hour. We then calculate *accumulated* excess electricity production for a country, see Figure 2 for Italy. In hours with positive excess production, the graph is increasing, whereas the graph is decreasing in hours with negative excess production. For hours with positive accumulated excess electricity, the graph is above the horizontal axis,

whereas the opposite is the case for hours with negative accumulated excess electricity. As seen from Figure 2, in the last hour accumulated excess electricity is zero, which simply reflects our restriction that over the period 2006-15, total intermittent production should be equal to total consumption.

Because a feasible electricity system requires equality of production and consumption in each point in time (here hour), we need to extend the electricity system with a storage technology, here batteries. We impose the following simple battery strategy:

i) If excess production is positive in an hour, load the battery
ii) If excess production is negative in an hour, discharge the battery provided there is stored electricity in the battery
iii) If excess production is negative in an hour, but there is no stored electricity in the battery, use a back-up technology to ensure that total production (from intermittent electricity and the back-up technology) is equal to consumption.

We use this battery strategy for each of the 23 countries when there is no trade in electricity, as well as for EU-23.FB, and also when there is full trade in electricity between the 23 countries, henceforth termed EU-23.trade. For the latter case, we assume (for simplicity) that trade is never constrained by the capacity of international transmission lines for electricity. Hence, for each hour, we group countries into two categories, those having positive excess production in this hour and those have negative excess production. Excess production (in an hour) is defined as the difference between these two numbers.

We also take into consideration that batteries are not perfect, that is, there are various losses associated with batteries. Here, we focus on the two largest sources, that is, loss associated with charging a battery (10 percent) and self discharge (0.1 percent per month).

Using the derived optimal capacity shares as well as the optimal total intermittent capacity, the weather data and the battery strategy, we can simulate the evolvement of stored electricity in the battery, as well as calculate production from the back-up technology (if it is necessary to use this technology). Because the battery strategy is myopic and thus does not take intertemporal considerations into account, before we proceed we check whether it is possible to reduce stored electricity in the battery, provided that the (pre-determined) path of production from the back-up technology is not changed in any hour. We find that this is not possible.

Figure 3 shows the resulting graphs for stored electricity in the battery (black graph) and accumulated production from the back-up technology (red graph) in the case of full trade between the 23 countries. In hours where electricity is stored in the battery, the graph for the evolvement of stored electricity is increasing, whereas this graph is decreasing in hours where electricity is discharged from the battery. Finally, in hours where excess production is negative, but there is no stored electricity in the battery, the graph is flat. In these hours, there is production from the back-up technology; the graph showing accumulated production from the back-up strategy increases in these hours.

As seen from Figure 3, stored electricity in the battery peaks at 137 TWh. This number can be compared to annual average consumption of electricity in the 23 countries, which is 3039 TWh. Hence, in the most demanding hour in the period 2006-15, an amount of electricity corresponding to 5 percent of annual electricity consumption is stored. The corresponding figures for the single countries (when there is no trade) are shown in Figure 4; these vary between 7 and 28 percent with a mean equal to 12 percent.

Figure 5 provides information on average annual stored electricity relative to average annual consumption of electricity. As seen from Figure 4, for EU-23.trade the number is 15 percent, which is much lower than the number for single countries (without trade); these vary between 18 and 37 percent with a mean equal to 27 percent.

Figure 6 provides information on hourly charge into the battery (positive), and hourly discharged from the battery (negative) in the case of EU-23.trade when hourly charge and discharge are measured relative to average hourly consumption in EU-23. In the most demanding hours, hourly charge corresponds to around 150 percent of average hourly consumption, whereas hourly discharge corresponds to 100 of average hourly consumption. Note that these hours occur infrequently; the vertical axis in Figure 6 measures number of hours in the period 2006-15.

We now turn to production from the back-up technology, see Figure 3. For the period 2006-15, total production from this technology is almost 700 TWh, which corresponds to around 2 percent of total consumption. The corresponding shares for single countries (without trade) are shown in Figure 7; these vary between 3 and 5 percent. Because we have imposed that total intermittent production should be equal to total consumption over the period 2006-15, accumulated production from the back-up technology is equal to stored electricity in the battery in the last hour in 2015 plus accumulated losses in batteries.

Whereas the market share of the back-up capacity is low, its capacity is large (368 GW); if it is fully utilized, it will generate an amount of electricity that is slightly (6 percent) higher than average hourly consumption in EU-23. The reason is simply that the back-up capacity has to be able to handle hours with low intermittent production and high load.

4 Robustness

In this section we test the robustness of the results obtained in Section 3 with respect to i) imposed total intermittent production relative to total consumption in the period 2006-15, ii) sequence of weather and load characteristics in the ten years period under study, and iii) which cells that are developed for intermittent production.

Level of intermittent production

In the reference case, we imposed that for the entire 2006-15 period total intermittent production should equal total consumption of electricity for each country. Assume, alternatively, that intermittent capacities are chosen under the restriction that total intermittent production should exceed total consumption. If, for example, total intermittent production exceeds consumption by 20 percent, we find that the optimal capacity shares are almost identical to the ones in the reference scenario. This result reflects that by assumption, total capacity of a technology is spread evenly between the 10 percent best cells, and the productivity of each cell (β_t^i) is constant, that is, independent of the capacity installed.

However, more intermittent production has of course impact on the need for back-up production and also on the amount of electricity stored in the batteries. Let λ measure imposed total intermittent production relative to total consumption in the period 2006-15 ($\lambda = 1$ in the reference scenario). Figure 8 shows the relationship between this parameter and total back-up production. As expected, a higher value of λ lowers back-up production. In particular, for λ exceeding 1.43, there is no need for a back-up technology.

If the parameter λ is increased further, at least as a rule of thumb, the amount of electricity stored in the batteries decreases. In order to avoid any storage of electricity in the batteries, λ has to be as high as 10.73. This reason is simply that over the 10-year period 2006-15, there are several demanding hours with little wind/solar irradiance and high load.

Sequence of years

In the reference case, we followed true time over the period 2006-15. The sequence of years may be important because in the first hour of the 10-year period, per assumption there is no stored electricity in the battery. If the start of the first year is characterized by low wind/solar irradiance or high load, there will be demand for back-up production and hence no electricity will be stored in the battery.

We now test the importance of the sequence of years by Monte Carlo simulations: We draw one year from a distribution over the 10 years in the period 2006-15. This will be our first year in a 10-year sequence. We repeat this procedure 10 time, and thus obtain a specific sequence of 10 years. We then draw a new sequence of 10 years, and continue until we have 100.000 sequences Because we always draw from the distribution over the years in the period 2006-15, most sequences contain less than 10 distinct years.

For each sequence, we undertake the exercise described in Section 3, and thus obtain variables for maximum stored electricity in an hour, average annual stored electricity in the batteries, average annual production from the back-up technology, and capacity of the back-up technology. Panels a-d in Figure 9 show histograms of these four variables, and also report their average value; they are 144 TWh (maximum stored electricity in an hour), 465 TWh (annual stored electricity), 61 TWh (annual backup production), and 362 (backup capacity). These averages do not differ much from the corresponding values in the reference case in Section 3.

Top cells

In the reference case, investment in capacity of an intermittent technology is spread out evenly between its 10 percent top cells. However, even among these cells there is a significant difference in productivity (β_t^i). An alternative assumption is that for each technology, first development takes place in the best cell, then in the second best cell, etc. With such a cost-efficient rule, one has to decide how much capacity that can be developed in a cell.

In the reference case, for most countries installed capacity of an intermittent technology varies between 2.5 GW and 12.5 GW per cell. In the Appendix, we discuss land requirement per MW installed capacity for wind parks and solar parks. With our estimates, between 1 percent

(corresponding to 2.5 GW) and 5 percent (corresponding to 12.5 GW) of the land in an onshore cell is used for development of an intermittent technology in the reference case.

We now redo the exercise in Section 3 ($\lambda = 1$) under the alternative assumption of cost-efficient development. First, we impose that 2.5 GW capacity can be installed in each cell. Then the cap is increased to 12.5 GW. For both caps, we draw 20.000 sequences of 10 years, see the procedure above. Figures 10 and 11 show the resulting histograms for a 2.5 GW cap and a 12.5 GW cap, respectively. Each figure contains four panels; maximum stored electricity in an hour, annual stored electricity in the batteries, annual production from the back-up technology, and capacity of the back-up technology. These can be compared to the corresponding panels in Figure 9 where the 10 percent best cells are developed. Overall, we find moderate differences between the three cases.

5 Concluding remarks

Using re-analysis data for the period 2005-16 and simulations, we have shown how Europe can design an electricity generation sector where around 98 percent of total production is generated by wind power and solar. In our reference case, a large amount of batteries must be installed to make the system work. In the most demand hour in the period 2006-15, an amount of electricity corresponding to 5 percent of average annual consumption of electricity has to be stored in the batteries. Average annual use of batteries corresponds to 15 percent of average annual consumption of electricity. Note that these numbers are for the case of 23 European countries trading in electricity. Without any trade, the numbers for single countries are much larger.

Throughout the paper, we have referred to a flexible backup technology to be used in periods with low wind/solar irradiance, high load and no electricity stored in the battery. What are the emissions from this technology? If this technology is bio power, and we follow the standard assumption in energy market modelling, there are no GHG emissions. However, an alternative view is that emissions from bio power are substantial, and may be comparable to coal power, see, for example, Haberl et al. (2012). If so, thermal power with CCS could serve as the backup technology. Such a technology will meet the EU target of a 95 percent emissions reduction if its market share is 2 percent.

While we have assumed that existing electricity capacities are not used in the constructed electricity generation sector, application of existing nuclear and hydro capacities in the constructed electricity system will lower demand for storage. For example, assume that hourly nuclear production is constant over time (existing nuclear plants can hardly change their production over the day), and that their share of total production is 25 percent, which was the case in the EU in 2015. Then maximum battery capacity is lowered from 137 TWh (reference case) to 107 TWh, whereas annual battery usage is lowered from 459 TWh (reference case) to 343 TWh.

On the other hand, the EU goals of radical emissions reductions (40 percent by 2030 and 80 percent by 2050) may require (partial) electrification of several activities, for example, transportation, heating and cooking. Thus, over time demand for electricity will increase in Europe. Assume that the generated effect is an increase in hourly electricity demand by 50 percent of average hourly consumption (in all 23 countries, in all years, in all hours). Then maximum battery capacity is increased from 137 TWh (reference case) to 222 TWh, whereas annual battery usage is increased from 459 TWh (reference case) to 702 TWh.

However, we may also use the existing hydro capacity (in addition to nuclear plants) in the constructed electricity system, and take advantage of the fact that reservoir hydro and pumped storage hydro are flexible technologies with respect to hourly and seasonal production profiles. Typically, the amount of water in reservoirs reaches a minimum in the spring and a maximum in the fall. By postponing half of the hydro production from the spring to the fall, using existing nuclear capacities, but also take a 50 percent increase in demand for electricity into account, maximum battery capacity is found to be 137 TWh, that is, the same number as in the reference case. This suggests that the EU may be able to handle its climate targets mainly through a combination of expansion of wind and solar power, massive investment in batteries, and use of the existing nuclear and hydro capacities.

Figure 1 Optimal capacity shares in intermittent technologies

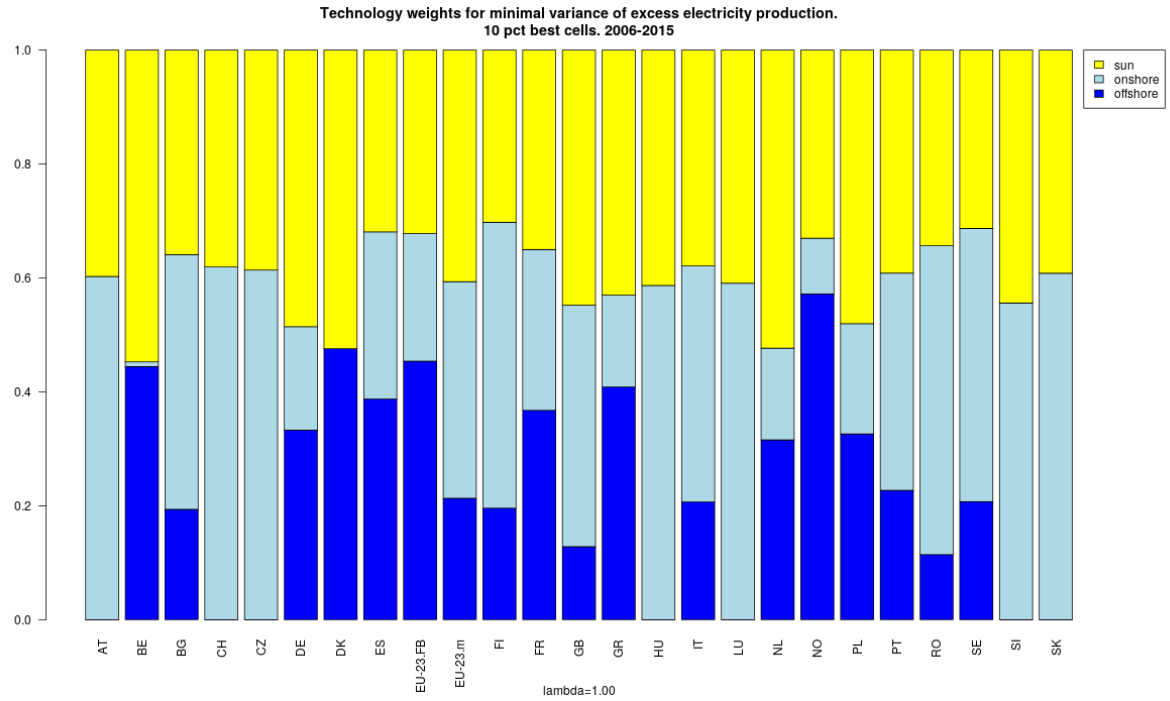
Technology weights for minimal variance of excess electricity production.
10 pct best cells. 2006-2015
sun
onshore
offshore
1.0
0.8
0.6
0.4
0.2
0.0
AT
BE
BG
CH
CZ
DE
DK
ES
EU-23.FB
EU-23.m
FI
FR
GB
GR
HU
IT
LU
NL
NO
PL
PT
RO
SE
SI
SK
lambda=1.00

Figure 2 Accumulated excess electricity production in Italy

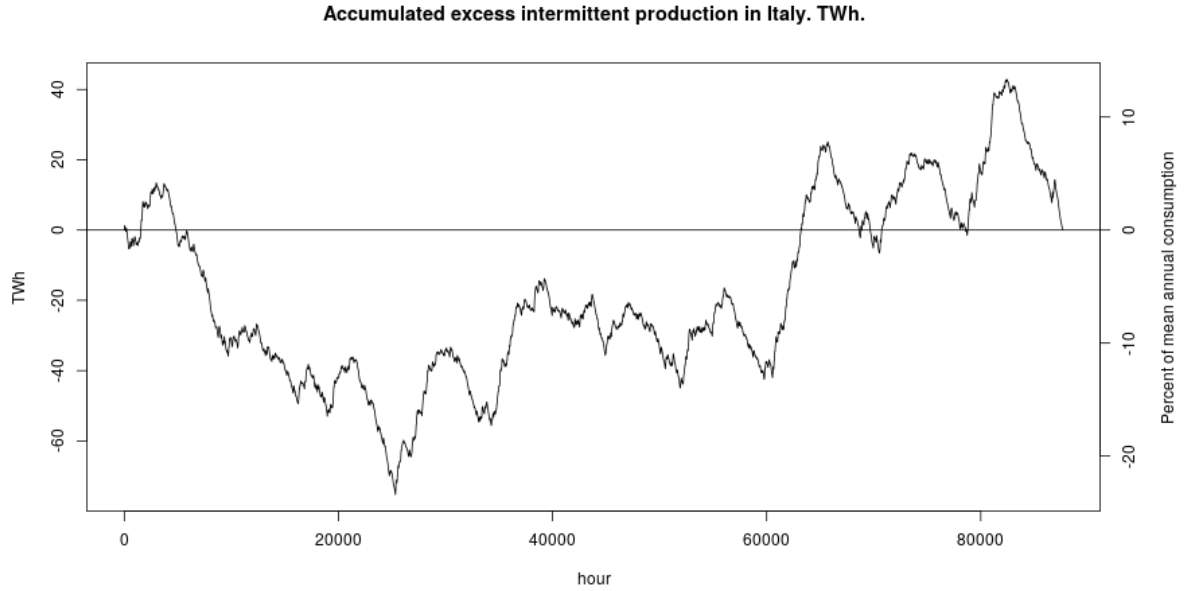

Figure 3 Battery capacity and accumulated back-up production. 23 countries with trade.

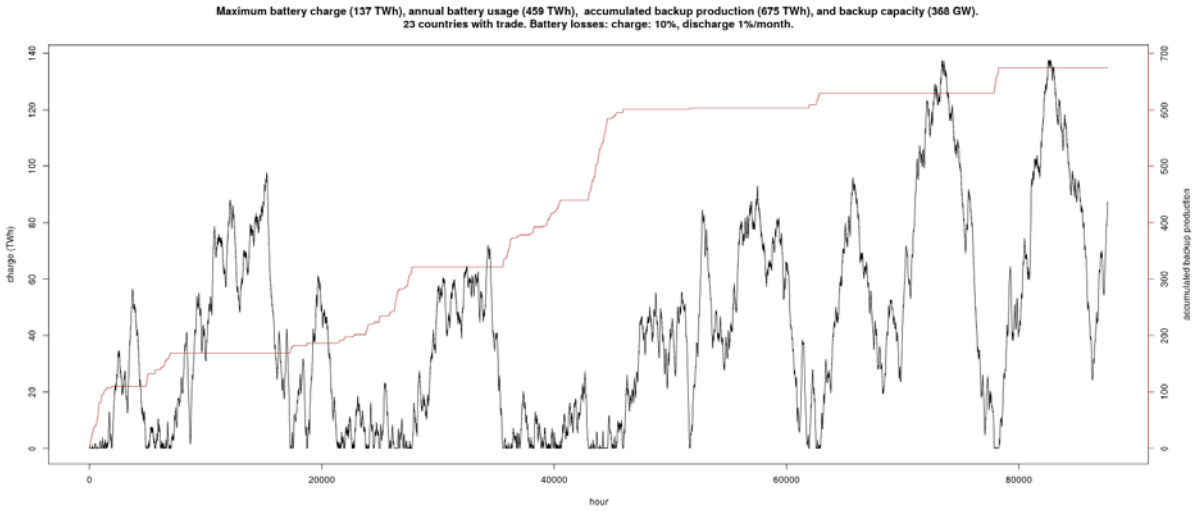

Figure 4 Battery capacity as a percentage of average annual consumption

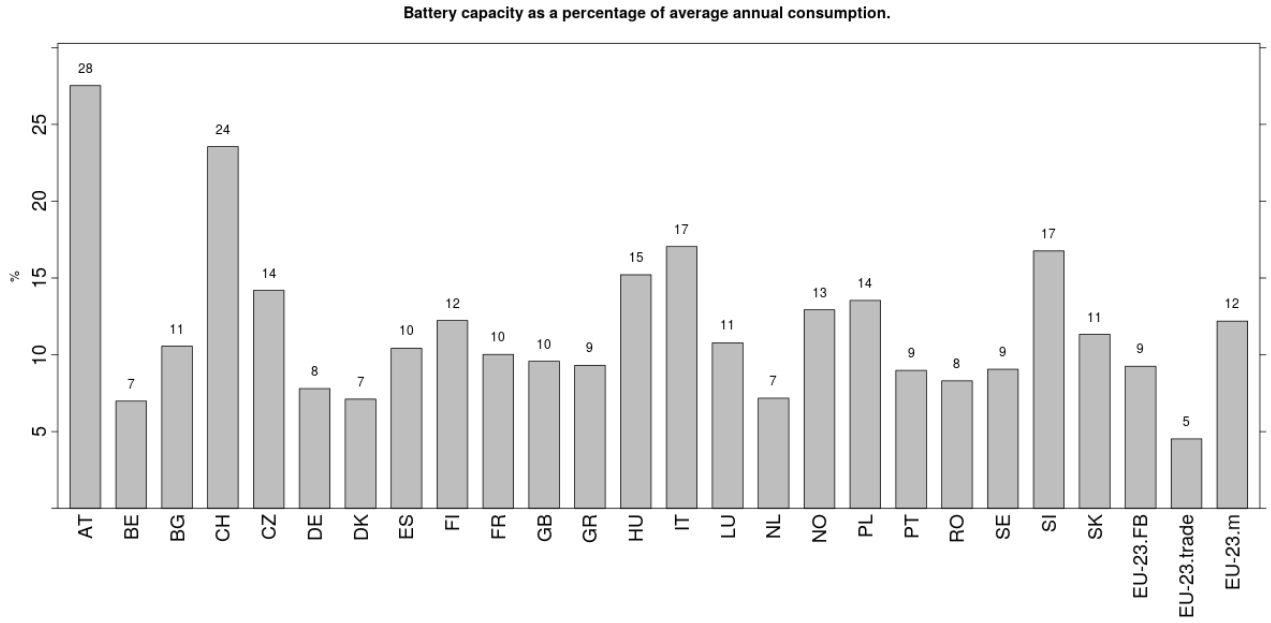

Figure 5 Average annual battery use as a percentage of average annual consumption

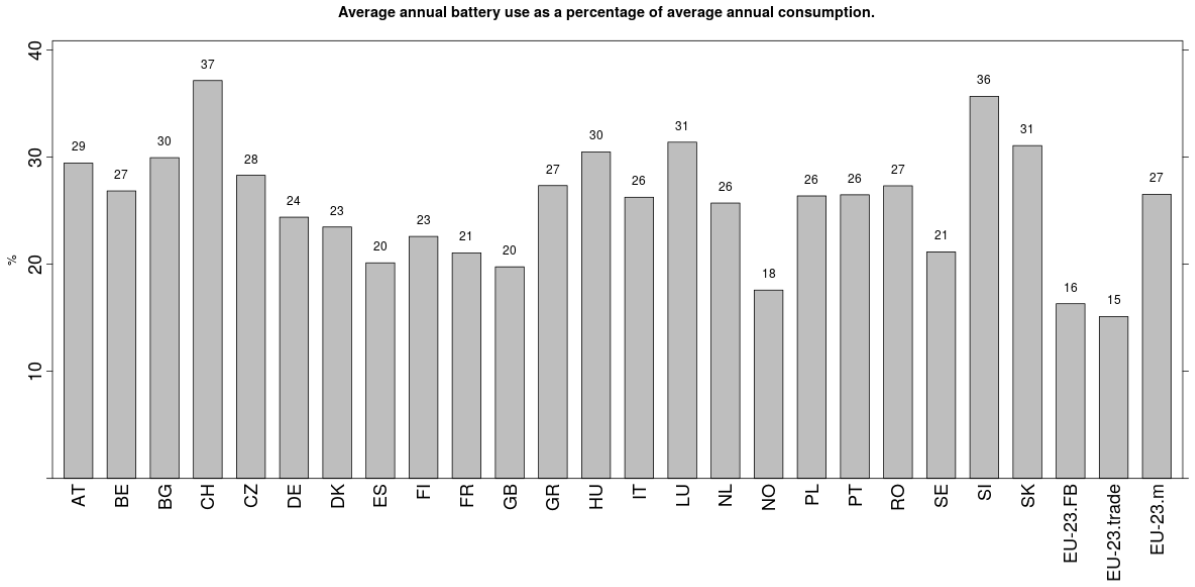

Figure 6 Historgram of charge and discharge measured as percentage of average hourly consumption. 23 countries with trade.

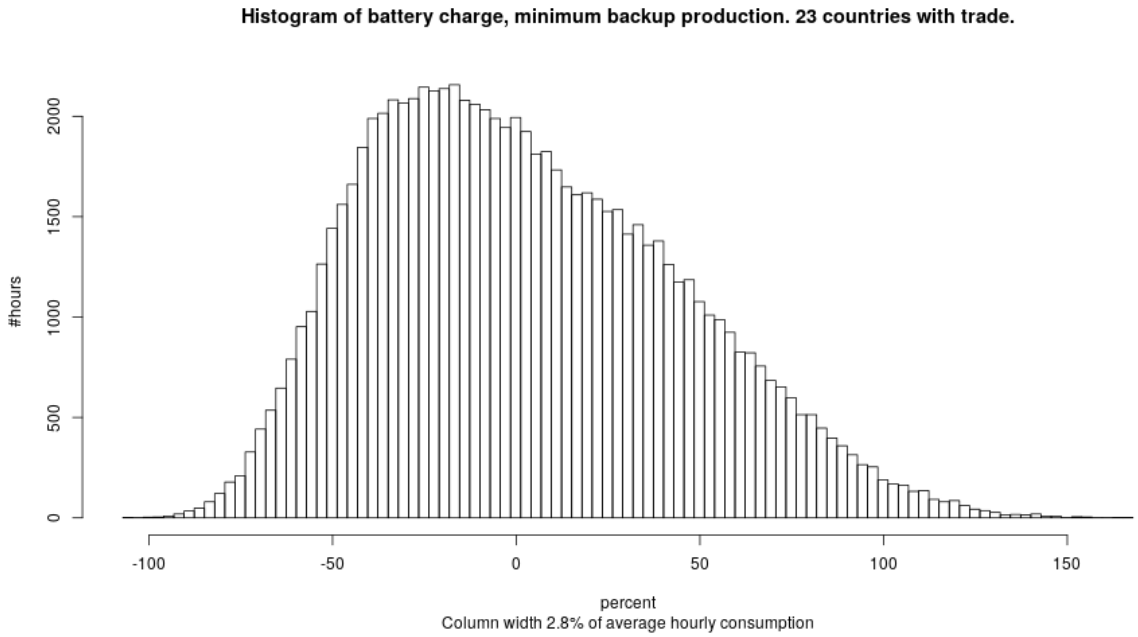

Figure 7 Average annual production from the back-up technology relative to average annual consumption.

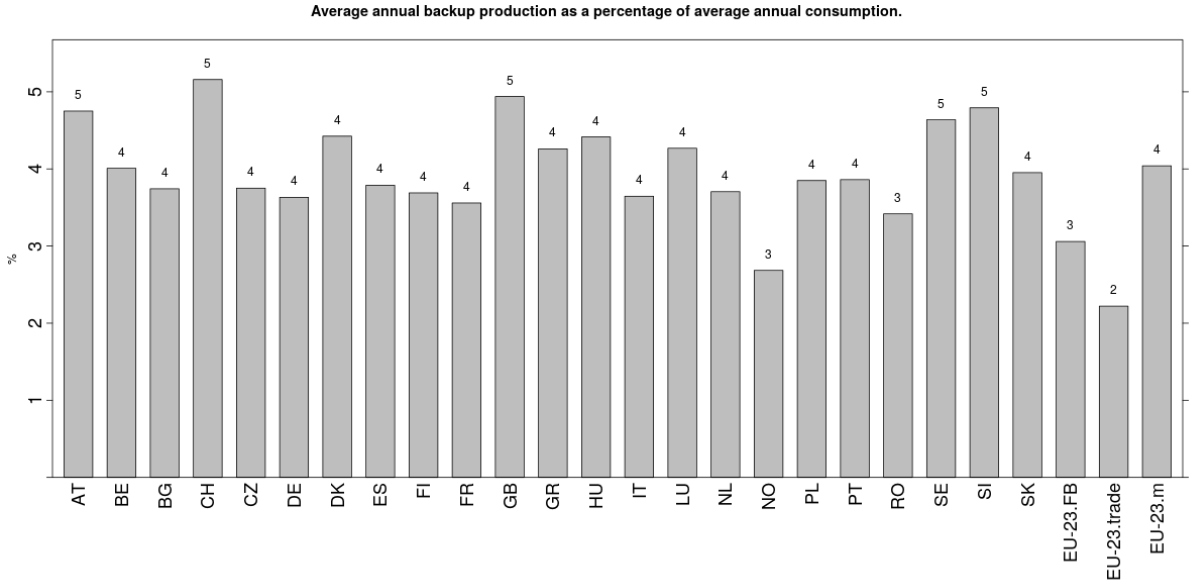

Figure 8 Annual battery use and backup production. 23 countries with trade.

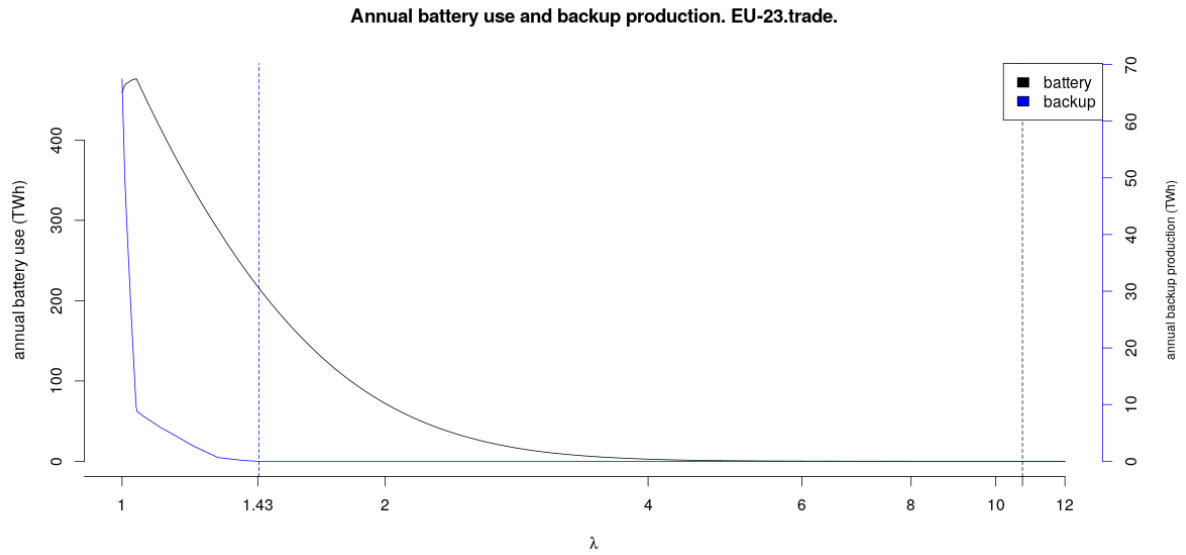

Figure 9 Monte Carlo Simulations when top 10 percent cells are developed for intermittent production. 23 countries with trade.

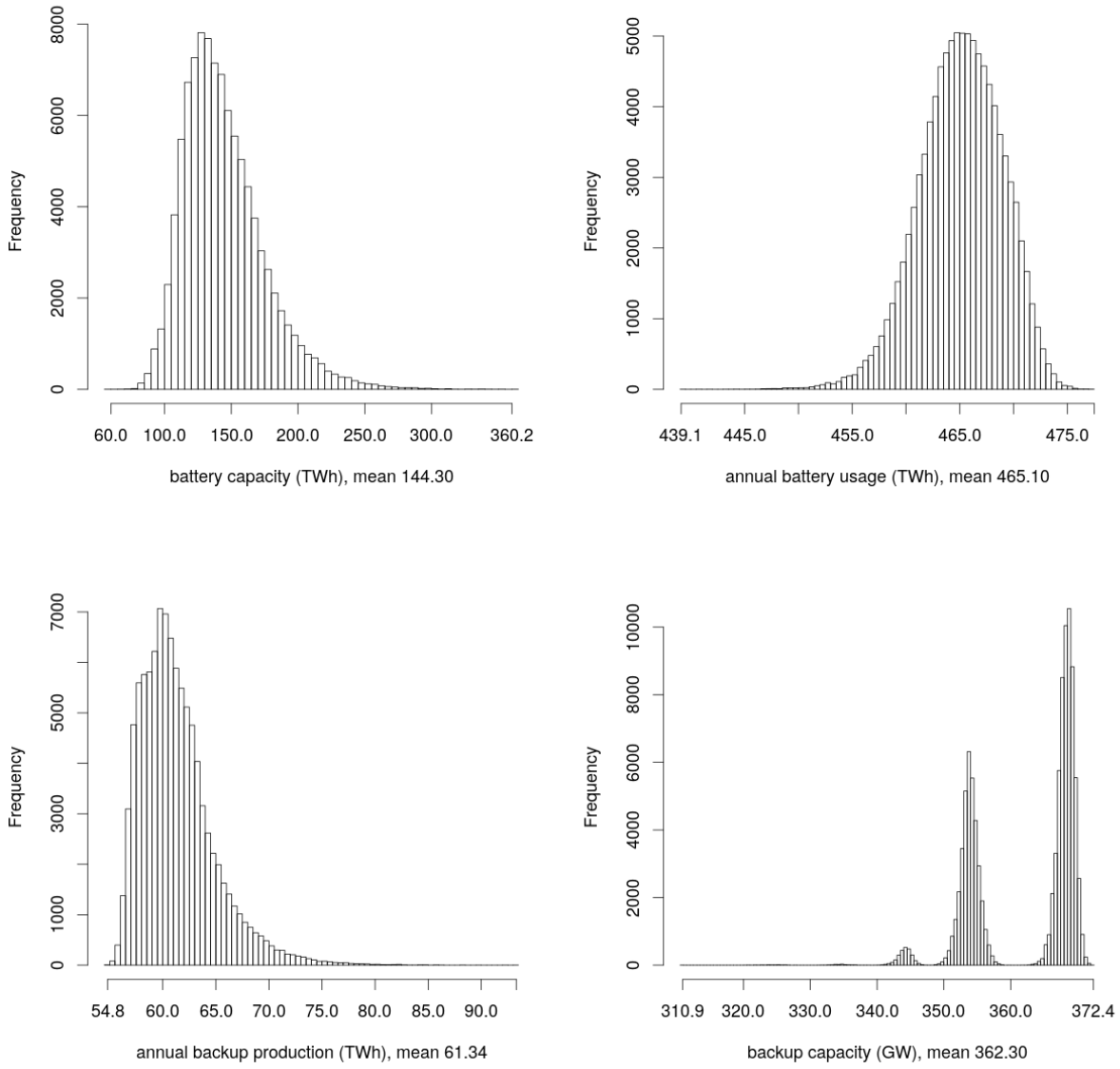

Figure 10 Monte Carlo Simulations with cost-efficient development of intermittent production and cap in each cell is 2.5 GW. 23 countries with trade.

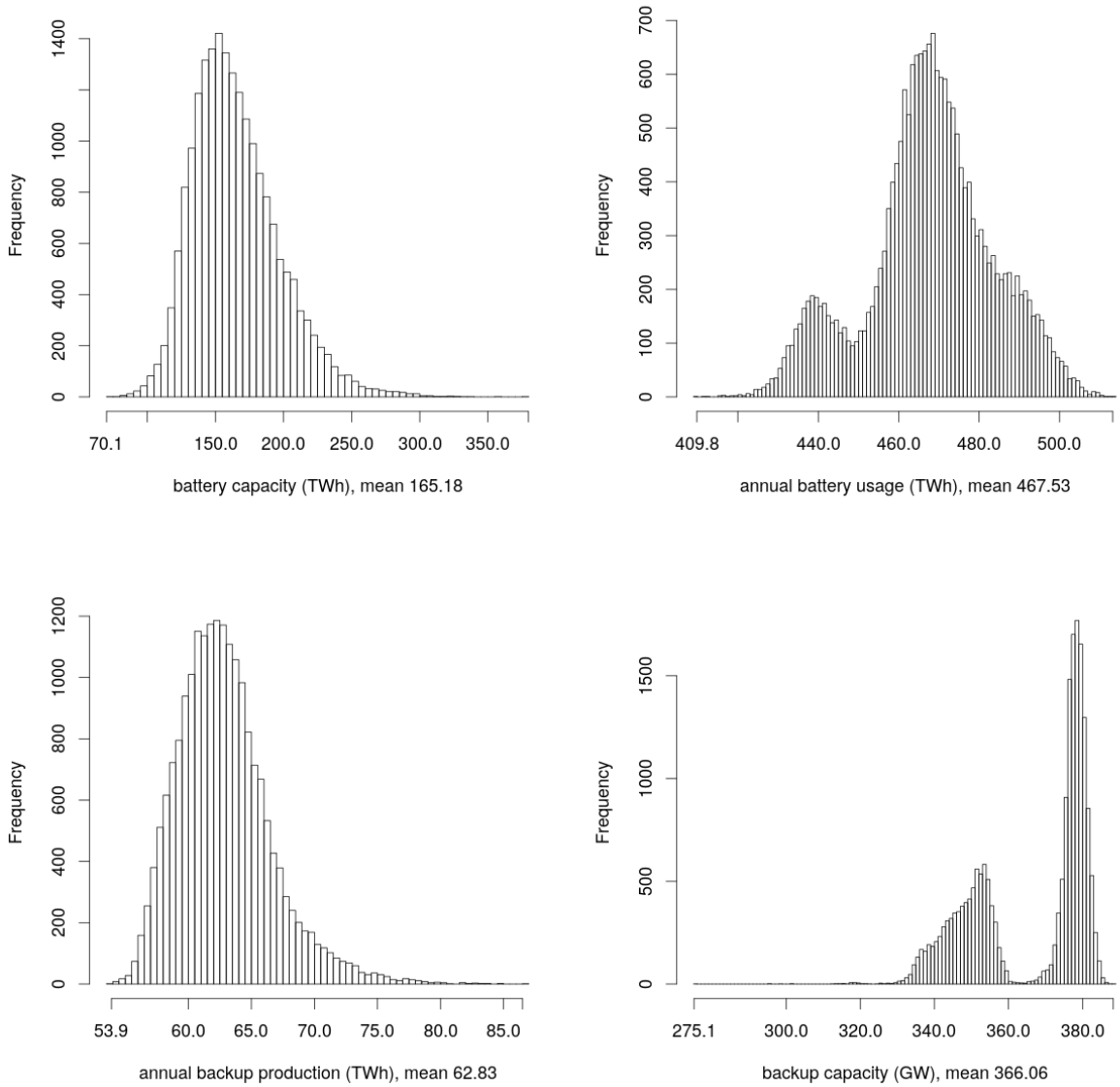

Figure 11 Monte Carlo Simulations with cost-efficient development of intermittent production and cap in each cell is 12.5 GW. 23 countries with trade.

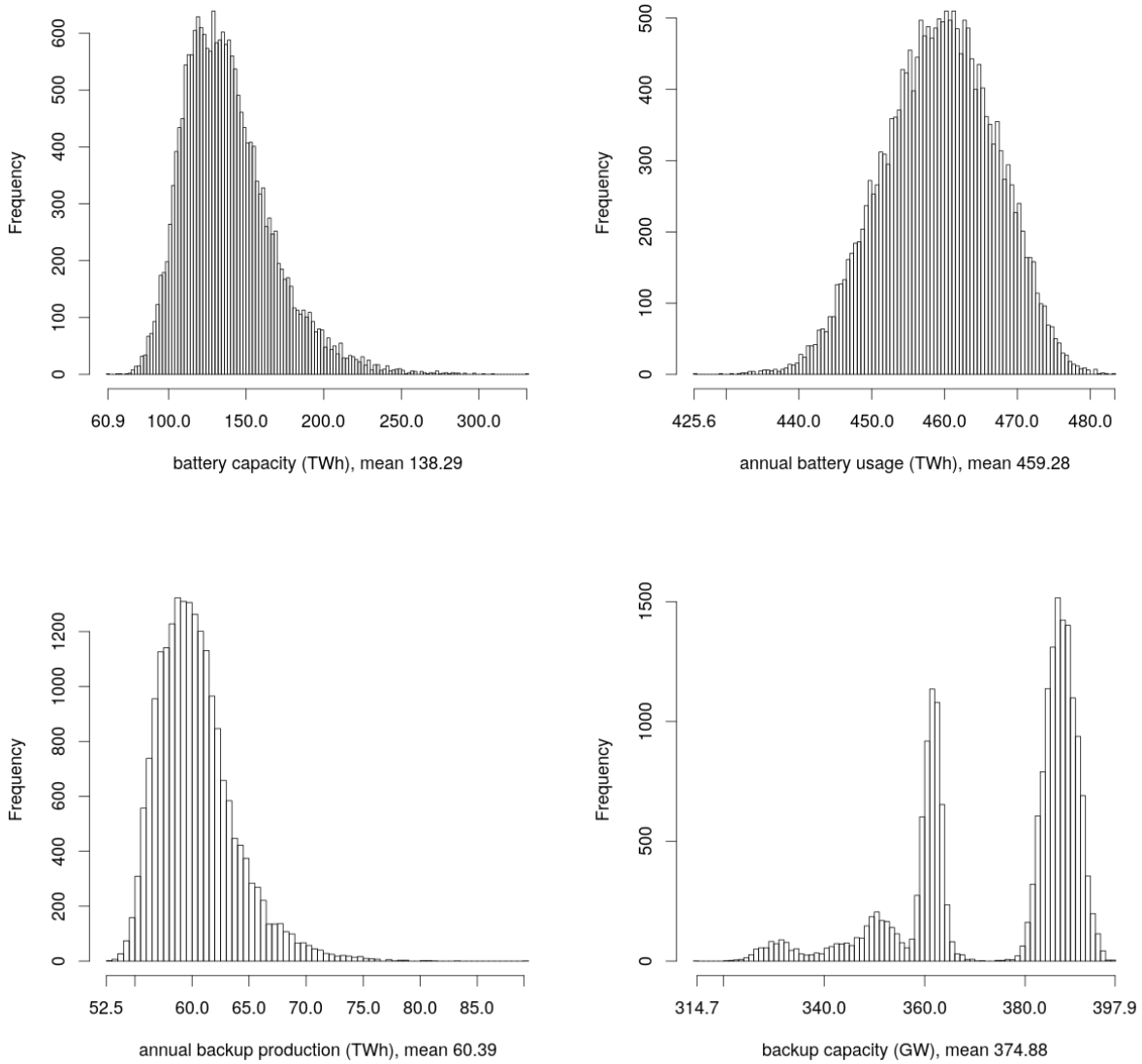

References:

Breyer, C., Bogdanov, D., Aghahosseini, A., Gulagi, A., Child, M., Oyewo, A. S., Farfan, J. and K. Sadovskaia (2017). Solar photovoltaics demand for the global energy transition in the power sector. Progress in photovoltaics: Research and applications, 1-19.

Clack, C. T. M., Qvist, S. A., Apt, J., Bazilian, M., Brandt, A. R., Caldeira, K., Davis, S. J., Diakov, V., Handschy, M. A., Hines, P. D. H., Jaramillo, P., Kammen, D. M., Long, J. C. S., Morgan, M. G., Reed, A., Sivaram, V., Sweeney, J., Tynan, G. R., Viktor, D. G., Weyant, J. P. and J. F. Whitacre (2017). Evaluation of a proposal for reliable low-cost grid power with 100% wind, water, and solar. PNAS, Vol. 114 (26), 6722-6727.

Elliston, B., Diesendorf M. and I. MacGill (2012). Simulations of scenarios with 100% renewable electricity in the Australian national electricity market. Energy Policy, Vol. 45, 606-613.

Elliston, B., Diesendorf M. and I. MacGill (2014). Comparing least cost scenarios for 100% renewable electricity with low emission fossil fuel scenarios in the Australian national electricity market. Renewable Energy, Vol. 66, 196-204.

Gelaro, R., McCarty, W., Suárez, M.J., Todling, R., Molod, A., Takacs, L., Randles, C.A., Darmenov, A., Bosilovich, M.G., Reichle, R., Wargan, K., Coy, L., Cullather, R., Draper, C., Akella, S., Buchard, V., Conaty, A., Da Silva, A.M., Gu, W., Kim, G-K., Koster, R., Lucchesi, R., Merkova, D., Nielsen, J.E., Partyka, G., Pawson, S., Putman, W., Rienecker, M., Schubert, S.D., Sienkiewicz, M. and B. Zhao (2017). MERRA-2, Journal of Climate, Vol. 30, 5419-5454. DOI: 10.1175/JCLI-D-16-0758.1

Haberl, H., Sprinz, D., Bonazountas, M., Cocco, P., Desaubies, Y., Henze, M., Hertel, O., Johnson, R. K., Kastrup, U., Laconte, P., Lange, E., Novak, P., Paavlola, J., Reenberg, A., van den Hove, S., Vermeire, T., Wadhams, P. and T. Searchinger (2012). Correcting a fundamental error in greenhouse gas accounting related to bioenergy. Energy Policy, Vol. 45, 18-23.

Jacobson, M. Z., Delucchi, M. A., Cameron, M. A. and B. A. Frew (2015). Low-cost solution to the grid reliability problem with 100% penetration of intermittent wind, water, and solar for all purposes. PNAS, Vol. 112 (49), 15060-15065.

Koskinen, O. and C. Breyer (2016). Energy storage in global and transcontinental energy scenarios: A critical review. Energy Procedia, Vol. 99, 53-63.

Mai, T., Mulcahy, D., Hand, M. M. and S. F. Baldwin (2014). Envisioning a renewable electricity future for the United States. Energy, Vol. 65, 374-386.

Rasmussen, M. G., Andresen G. B. and M. Greiner (2012). Storage and balancing synergies in a fully or highly renewable pan-European power system. Energy Policy, Vol. 51, 642-651.

Salomon, A. A., Bogdanov, D. and C. Breyer (2018). Solar driven net zero emission electricity supply with negligible carbon cost: Israel as a case study for Sun Belt countries. Energy, Vol. 155, 87-104.

Searchinger, T. D., Beringer, T. and A. Strong (2017). Does the world have low-carbon bioenergy potential from the dedicated use of land? Energy Policy, Vol. 110, 434-446.

Sgouridis, S., Csala D. and U. Bardi (2016). The sower's way: quantifying the narrowing net-energy pathways to a global energy transition. Environmental Research Letters, Vol. 11, 1-8.

Sinn, H.-W. (2017). Buffering volatility: A study on the limits of Germany's energy revolution. European Economic Review, Vol. 99, 130-150.

Appendix. Solar and wind data.

Contents

List of Figures

A.1 Raw data

We have fetched data from three MERRA-2 databases at `https://disc.sci.gsfc.nasa.gov/datasets?keywords="MERRA-2"`, called `tavg1_2d_slv_Nx`, `tavg1_2d_rad_Nx`, and `tavg1_2d_flx_Nx`. Henceforth referred to as `slv`, `rad`, and `flx`. We have fetched data from the period 2006-01-01 to 2015-12-31. The variables are:

- `swgdn` is shortwave incident flux on the ground, i.e. the solar flux on a horizontal plane in the spectrum 175-3800 nm (W/m^2). From dataset `rad`.
- `swtdn` is shortwave incident flux at top of atmosphere. From dataset `rad`.
- `albedo` is full spectrum albedo of the earth's surface. From dataset `rad`.
- `u50m`, `v50m` are east- and northwards wind speed component at 50m height (m/s). From dataset `slv`.
- `t2m` is temperature at 2m height (Kelvin). Converted to Celsius by subtracting 273.15. From dataset `slv`.
- `z0m` is the surface roughness coefficient (m). From dataset `flx`.
- `rhoa` is the air density at ground level (kg/m^3). From dataset `flx`.

The MERRA-2 data are organized along three dimensions; a 2d-grid with latitude resolution 0.5 degrees and longitude resolution of 5/8 degrees, and time by hour. The data in the `tavg1`-datasets are averaged over time and over each grid-cell, with the lat/lon-coordinate being the centre of the cell. The time is in UTC, the start of each 1-hour period.

We then assign a country and an offshore/onshore status to the cells as follows. We use offshore zones downloaded from `http://www.marineregions.org/` (Maritime Boundaries). We use offshore zones which are designated as internal waters or within 12 nautical miles from shore. If the grid cell overlaps an offshore zone, we assign it as offshore to that country. It is possible that a cell is offshore to more than one country; in that case we choose one of them. Otherwise, if the centre of the cell lies onshore in a country as determined by R-package sp [9], with the high resolution map available in R package rworldxtra [11], we assign it to that country. The cells which have not been assigned to a country are discarded. Figure 1 depicts the onshore and offshore cells we use.

A.2 Variable transformations

A.2.1 Wind

We need the scalar wind speed at 100m since MERRA-2 does not provide wind at 100m. First we compute the wind speed at 50m as $v_{50} = (\texttt{u50m}^2 + \texttt{v50m}^2)^{1/2}$.

Then we use the logarithmic wind profile law, found e.g. in [2],

$$v_h = v_0 \frac{\log(h/z_0)}{\log(h_0/z_0)},$$

where v_h is wind speed at height h, v_0 is wind speed at height h_0, and z_0 is the surface roughness coefficient. This is the MERRA-2 variable `z0m`. We can now compute the wind speed at height 100 m as

$$v_{100} = v_{50} \frac{\log(100/z_0)}{\log(50/z_0)}.$$

The output of a wind turbine depends on several factors. The rated power is typically specified at an air density of 1.225 kg/m^3, which is the density of dry air at 15 °C at

Figure 1: Onshore and offshore cells

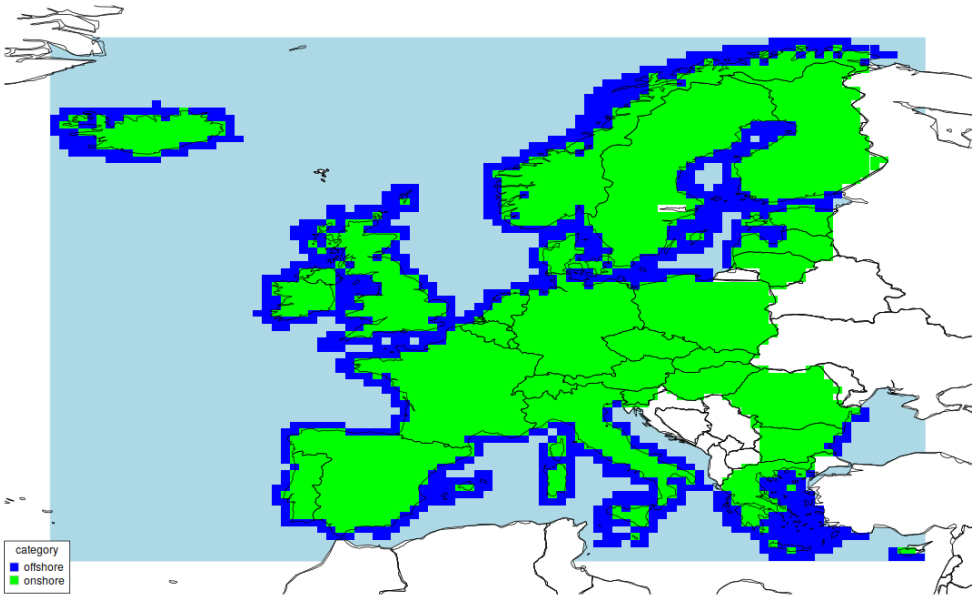

a standard pressure of 101.325 kPa. The wind energy is proportional to the density, which varies with pressure, temperature and humidity. We compute a density factor as $\rho = \texttt{rhoa}/1.225$. That is, we somewhat inaccurately assume the same factor applies at a height of 100 m.

To find the output power relative to the rated power, which is a function of the wind speed $C(v)$, we can use a cubic power curve. Its shape is determined by three parameters. The wind speed is adjusted with the density so that $v = \rho^{1/3} v_{100}$.

The simplest power curve is determined by three parameters; a cut-in speed v_i, a rated speed v_r, and a shut-off speed v_z:

$$C(v) = \begin{cases} 0 & \text{for } v < v_i, \\ \left(\frac{v - v_i}{v_r - v_i}\right)^3 & \text{for } v_i \le v \le v_r, \\ 1 & \text{for } v_r < v < v_z, \\ 0 & \text{for } v \ge v_z. \end{cases}$$

More realistically, a sigmoid cubic can be used, based on the S-shaped graph of the function $f(x) = 3x^2 - 2x^3$. We add an additional parameter v_o, and let the power go smoothly to 0 when wind is stronger than v_o:

$$S(v) = \begin{cases} 0 & \text{for } v < v_i, \\ 3\left(\frac{v - v_i}{v_r - v_i}\right)^2 - 2\left(\frac{v - v_i}{v_r - v_i}\right)^3 & \text{for } v_i \le v \le v_r, \\ 1 & \text{for } v_r < v < v_o, \\ 1 - 3\left(\frac{v - v_o}{v_z - v_o}\right)^2 + 2\left(\frac{v - v_o}{v_z - v_o}\right)^3 & \text{for } v_o \le v \le v_z, \\ 0 & \text{for } v \ge v_z. \end{cases}$$

For a selection of wind farms, we have estimated farm curves from the MERRA wind by finding the v_i, v_r, v_o and v_z which minimize $\sum_i |m_i - p_i|^2$, with p_i being actual

Figure 2: Power curves

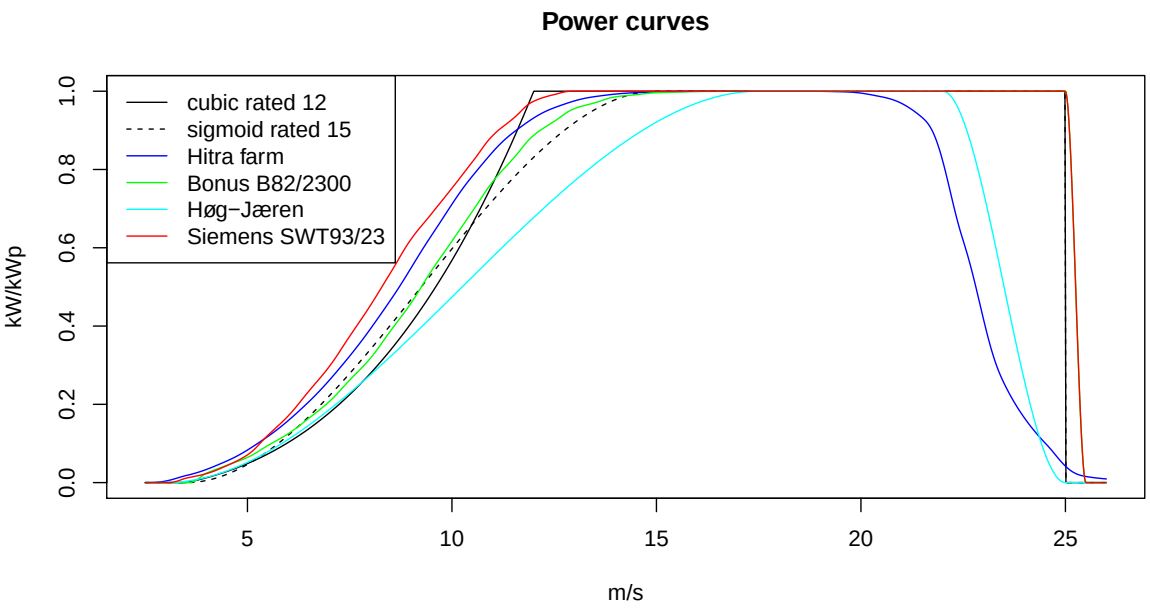

production in hour i, and m_i is modeled production with a sigmoid cubic and MERRA wind. The i ranges over the three years 2013–2015.

Figure 2 shows six power curves: a $C(v)$ for $v_r = 12$, a $S(v)$ for $v_r = 15$, two curves for actual wind farms, and power curves of the standalone turbines used in the farms (Bonus for Hitra, Siemens for Høg-Jæren). The standalone power curves are interpolated from `http://en.wind-turbine-models.com/powercurves`, whereas the power curves for the farms have been lifted from NVE Rapport 20/2014, appendix C (`http://publikasjoner.nve.no/rapport/2014/rapport2014_20.pdf`).

The farm power curves have been estimated by NVE from a wake loss model, and a run of the WRF weather model from NCAR, with local topographical data. That is, its reference wind is not MERRA-2 wind speed, but wind speed at one or more particular points in the area, as computed by a particular run of WRF. It is therefore not directly comparable with our data. In particular, the Hitra farm uses Bonus 82/2300 turbines, but the farm power curve actually lies above the turbine's power curve. This is because the reference wind is taken at a place with less favourable wind conditions than the actual turbines. That is also the reason why the farm curve starts to decline long before the cut-out speed of the turbine.

In a real wind farm the power curve also depends on the wind direction. We have looked at data for a wind farm to compare a directional power curve to a fixed power curve. For the Hitra wind farm we do have production data, as well as modelled data with different power curves, both a directional one, and a direction-averaged one, and modelled production from NVE, which they use for analysis. The various power curves we have used is the turbine curve for the Bonus 82 turbine, the NVE provided fixed and directional power curves (NVE Rapport 20/2014), our own estimated power curve, and actual production. These are summarized in Figure 3. Our estimated power curve is in reasonable agreement with the actual annual production, we are however too low in

Figure 3: Hitra full hours

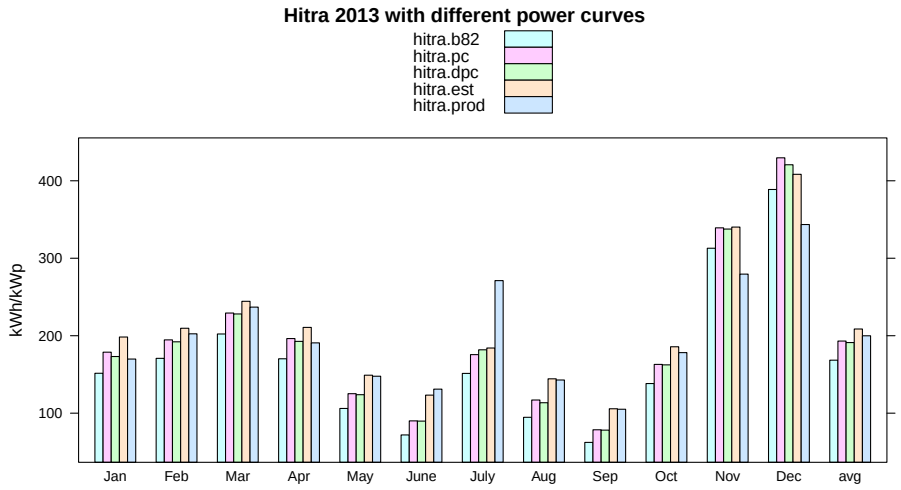

the summer, too high in the fall. We also see that there is little difference between the directional power curve and the fixed power curve. Thus, we do not attempt to model directional power curves.

We now take a look at individual hours for the Hitra wind farm in June 2013. The results are in figure 4. We have simulated production with our own estimated power curve, with the NVE provided farm power curve, and compare these to actual hourly production. Given that our geographical resolution is quite coarse, we think we are fairly close to the reality. However, the question remains, which farm curve to use in general.

In short, we have two systematic data problems with finding a generic power curve. The wind we have is averaged over a quite large area, whereas a wind farm typically will be placed where the wind is most favourable. But a wind farm will typically have some wake loss, which makes it less efficient than a single turbine. We do not have the capacity to model local topography to estimate the wind at the best sites, neither do we model output from existing wind farms like the EU EMHIRES project, and hence we settle for a single wind farm curve referenced to our MERRA wind.

To find a generic power curve, we have made a comparison between estimated power curves for a handful of Norwegian wind farms based on MERRA-2 wind in the nearest MERRA-2 grid cell. These are named Hitra, Smøla, Lista, Høg-Jæren, Raggovidda, and Bessakerfjellet. The results are shown in Figure 5. Typically, we estimate a v_i which is smaller than the turbine's v_i. This is probably because the wind is stronger in the farm than the averaged MERRA wind, so when MERRA wind is below the turbine's cut-in

Figure 4: Hitra wind farm, june 2013 by hour

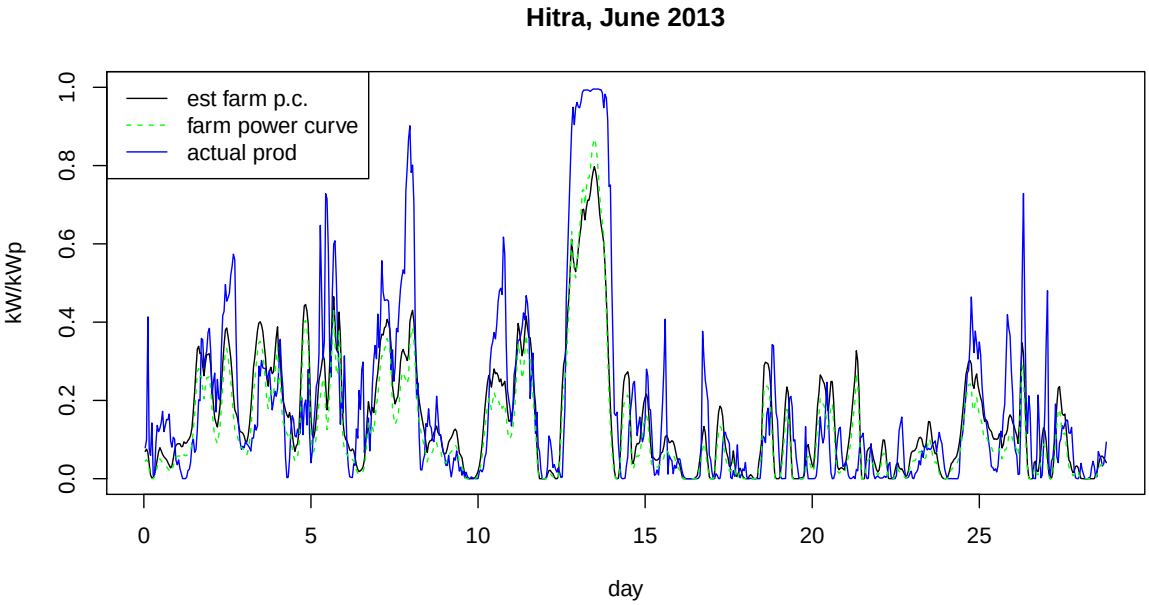

Figure 5: Estimated farm power curves

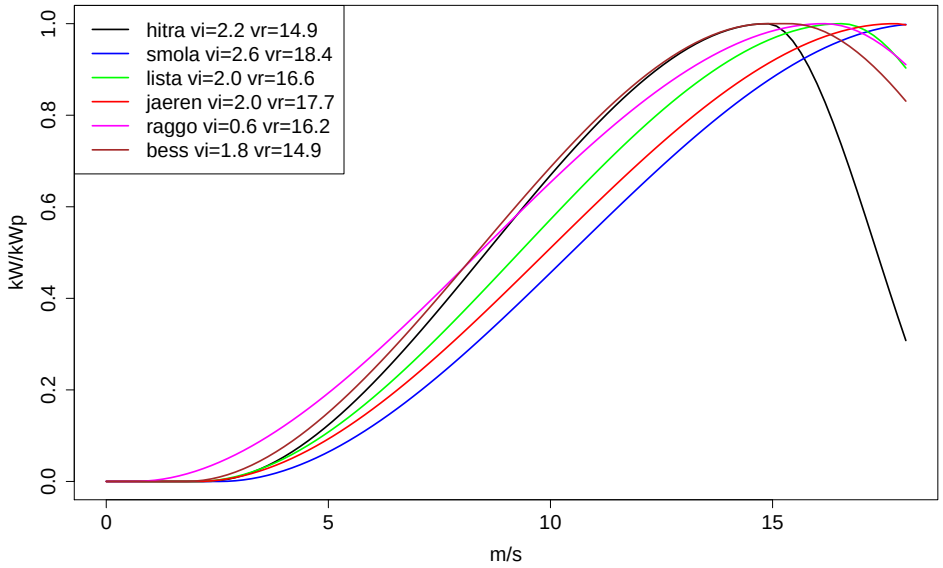

wind, the actual wind is above, so there is production. The estimated v_r is typically larger than the turbine v_r, which most likely is due to wake loss.

We have settled for a generic farm curve with $v_i = 3$, $v_r = 17.5$, $v_o = 22$, and $v_z = 25$. This is quite similar to parameters we estimate for the Høg-Jæren wind farm. With our generic power curve we match the aggregated capacity factor for Germany quite well, as can be seen in the EMHIRES comparison in section A.6. In addition, for the 10% best cells in Germany we simulate an annual average of 2658 full-load hours over the 10 year period 2006-2015, whereas expected full-load hours for wind turbines installed in Germany in 2018 is 2788 hours. [6]

A.3 PV

MERRA-2 does not have a variable for diffuse radiation, which we need when computing the insolation on a tilted solar panel. But we may estimate it from the ground radiation $r =$ `swgdn` and the top of atmosphere radiation $r_t =$ `swtdn` as follows. We first compute a *clearness index* as $k = \frac{r}{r_t}$. We then compute the diffuse fraction of the ground radiation as $d = (1 + \exp(-5.0033 + 8.6025k))^{-1}$, which is the simple model found in [3]. That is, direct radiation is $(1 - d)r$, and diffuse radiation is dr. Ideally, we should have used the more elaborate BRL-model from [7], but we do not have the required data.

The direction to the sun at a point in time at a certain place is computed by the R-package insol [4] as a unit vector n_s pointing toward the sun. The direct insolation on a tilted panel is computed as

$$R_d = (1 - d)r\frac{n_s \cdot n_p}{n_s \cdot n_z}$$

where n_p is an upward unit normal vector on the panel, and n_z is a zenith-pointing unit vector. Since we do not have access to local topographical data, we somewhat arbitrarily assume that the horizon is at a 5 degree inclination. This has the benefit that we avoid instability from excessively small denominators exactly at sunrise and sunset in the computation above, when n_s and n_z are nearly orthogonal.

A.3.1 Losses

Shadowing is critical for solar panels. Our typical module has an efficiency which goes linearly to 0 when the shadowed fraction goes to 2/3, i.e. a simple model of a module in landscape mode with few bypass diodes. In a solar farm with array-layout, the fraction of a module with direct radiation, i.e. the area above the shadow from the module-row in front, is

$$\psi = \max(0, \min(1, \mu\frac{n_s \cdot n_z}{n_s \cdot n_p})),$$

where μ is the horizontal distance between the rows in units of panel length (panel length is normalized to 1). The efficiency is therefore,

$$e = \max(0, \frac{3}{2}(\psi - 1/3)).$$

For standalone modules, we assume $e = 1$.

Figure 6 is a schematic of a solar farm seen from the east. We show three of the panel rows.

Figure 6: Solar farm schematic

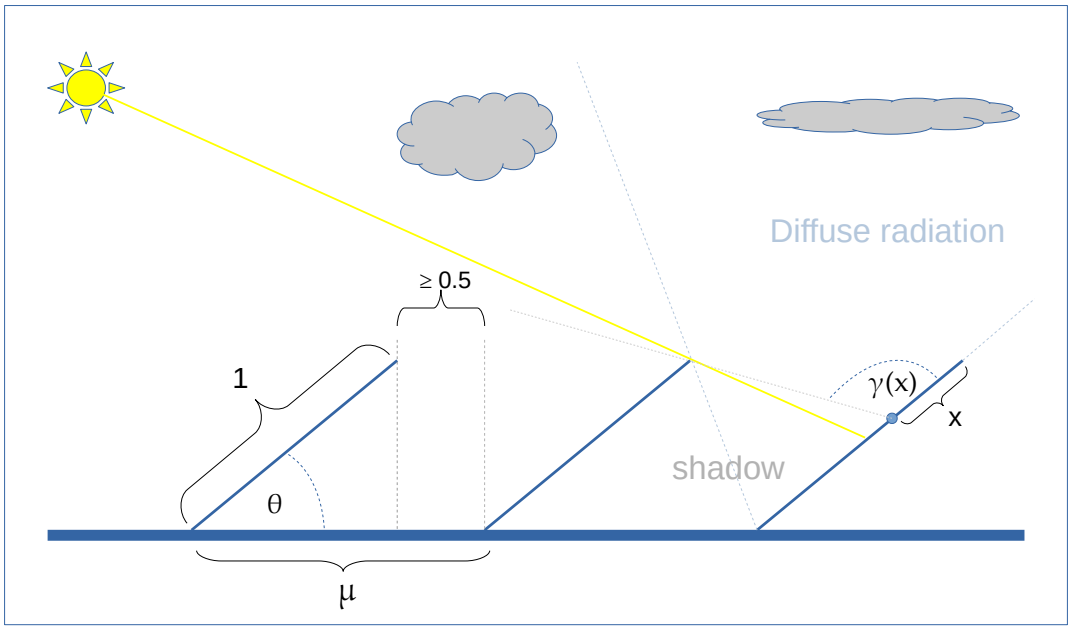

For standalone modules with tilt θ, the amount of isotropic diffuse radiation is,

$$R_f = dr(1 + \cos\theta)/2,$$

and the amount of reflected radiation from the ground is,

$$R_r = ar(1 - \cos\theta)/2,$$

where a is the albedo. For a solar farm with array layout and a common tilt, it's a bit more complicated. We compute the diffuse radiation as $R_f = \frac{1}{2}dr\int_0^1 1 - \cos(\gamma(x))\,dx$, where $\gamma(x)$ is the angle in Figure 6. By standard trigonometry, we have $\tan(\gamma(x)) = \frac{\mu\sin\theta}{x-\mu\cos\theta}$. A little care with which quadrant we are in, yields $\cos\gamma(x) = \frac{x-\mu\cos\theta}{\sqrt{x^2+\mu^2-2\mu x\cos\theta}}$. Integrating by substituting the radicand, tells us that,

$$R_f = \frac{1}{2}dr\left(1 + \mu - \sqrt{\mu^2 - 2\mu\cos\theta + 1}\right)$$

is the diffuse radiation. We assume that no reflected light reaches the module ($R_r = 0$).

These computations assume the horizon is at 0 degrees, and the farm is located in a horizontal plane area. In our solar farm calculations, we do not know the size (i.e. the number of rows) of the farm, so we assume all the rows (including the first) have the same amount of shadow.

For PV there are thermal losses which are incorporated as in [12]. That is, we have the ambient temperature at 2 m height from MERRA-2, $T_a = \texttt{t2m}$. We then compute the temperature on the panel as: $T_c = T_a + \frac{\texttt{NOCT}-20}{800}r_p(\theta)$, where

$$r_p(\theta) = R_d + R_f + R_r$$

is the flux on the panel (adjusted for a possible tilt θ), and we use the value $\texttt{NOCT} = 44$ [12]. Then the loss factor is,

$$\eta = 1 - \gamma_\ell(T_c - 25)$$

where γ_ℓ is the power temperature coefficient specific for the PV-module. We set $\gamma_\ell = -0.0037$.

A.3.2 Optimization

When optimizing the tilt θ we maximize total insolation, i.e. the sum of direct, diffuse and reflected radiation, adjusted for shadow inefficiency e and temperature η:

$$R(\theta) = \eta e r_p.$$

These quantities vary with time, so we index with the hour t and find the tilt angle which maximizes production over all the time periods:

$$\theta^* = \operatorname*{argmax}_\theta \sum_{t=1}^{N} R_t(\theta).$$

This is done separately in each of the grid cells to obtain a cell-specific optimal tilt angle.

For PV farms we maximize the total profit for a fixed area, over both the angle θ and the horizontal distance μ between the rows. Ideally, this should be done with endogenous prices, but we have settled for a fixed present value price of €100/MWh, and installation cost of €1000/kW with an annual discount rate of 4% over 25 years. We use a constraint $\mu - \cos\theta \geq 0.5$, so that there is room for half a panel between the rows. The vast majority of grid cells has a corner solution with minimal $\mu = 0.5 + \cos\theta$, though with varying tilt θ.

When optimizing profit we need the amount of produced energy, i.e. the power efficiency of the solar panel. From [12], we use the typical PV panel efficiency $\tau = 0.18$ at 25 °C.

In detail, in each cell we install one GW of solar panels and compute a profit per area $P(\theta, \mu)$ as a function of the angle θ and the distance μ: $P(\theta, \mu) = (p(1-L)\sum_t \tau R_t(\theta, \mu) - I)/\mu$, where I is discounted investment, p is the electricity price, and L is the system loss. We then optimize the θ and μ:

$$(\theta^*, \mu^*) = \operatorname*{argmax}_{\theta,\mu} \{P(\theta, \mu) \,|\, \mu \geq 0.5 + \cos\theta\}.$$

System losses, i.e. inverter loss, wiring, transformers etc. are $\approx 14\%$ according to `http://www.greenrhinoenergy.com/solar/technologies/pv_energy_yield.php`. That is, $L = 0.14$.

Note that if PV panels were free, and we did not need space between them for maintenance, the optimal farm would just cover the area with horizontal panels ($\mu = 1$ and $\theta = 0$), capturing all solar radiation in the area. Thus, if the size of the area is limited, it can be optimal to move panels as close as operationally possible and mount them relatively flat.

In the other direction, if land were unlimited, the rows of the solar farm could be spread arbitrarily far apart, effectively using the panels as standalone panels. This is reflected in our formulas in that if we let μ tend to infinity, the farm formulas converge to the standalone formulas.

A.4 Land use

When optimizing profit of PV-farms for a fixed area, we also compute the density of solar panels in the area. This varies with the location, though the general trend is that the area required for a particular installed effect grows somewhat with the latitude. We end up with a land use of typically 0.8 hectare per installed MW for most places in Europe, increasing in the far north.

Figure 7 is a box plot of the distribution of required land per installed MW for each country. We have removed some outliers for far north locations in Finland, Iceland and Norway, where solar farms are not profitable. The land requirement in ha/MW can be computed as $\mu/1.8$. In detail, a PV panel with efficiency 0.18 and capacity 1000 W has an area of $1/0.18$ m^2. So the area is $1000/0.18$ m^2 for 1 MW. But a PV panel in a particular farm uses a factor μ more of the ground area, so we use $1000\mu/0.18$ m^2/MW. Since a hectare is 10000 m^2, we end up with $\mu/1.8$ ha/MW.

Figure 7: Land use for PV

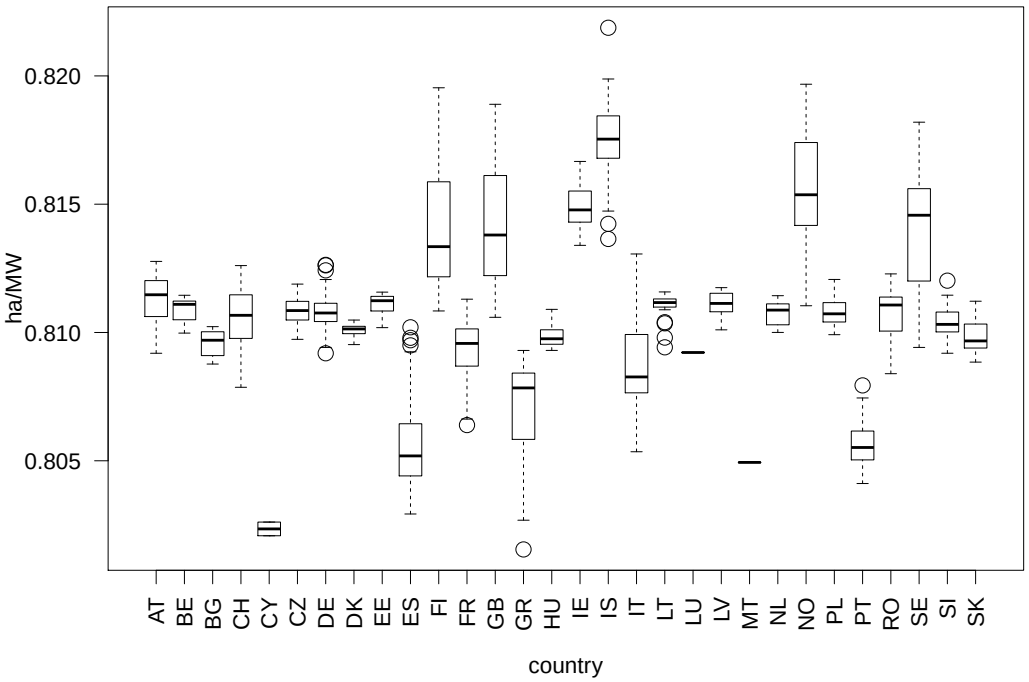

There is some infrastructure and various facilities associated with a solar farm, so we round up land use to 1 ha/MW. This means that 2.5 GW installed capacity of PV will use 1% of a grid cell in central Europe.

We have also made a rough estimate of land use by wind power. In the literature, two approaches are common: either the net land use (the turbines, access roads to the turbines, and other facilities) or the gross land use, the entire area of the wind farm.

REN21 [10] suggests that the net land use is 0.4 ha/MW. EWEA [1] suggests that the gross land use is 7 ha/MW (15 MW/km^2), with 1% of this being net land use. In [8], the gross figure 13–20 ha/MW is suggested for European wind farms (6-7 ha/MW is typical in California), with 1-3% (3-5% in the US) of this being net land use.

Figure 8: Land use for some wind farms

Site	Gross area	Installed effect	ha/MW	MW/km^2
Bessakerfjellet	3.5	57	6	16
Hitra 2	18	94	19	5
Høg-Jæren	6	73	8	12
Raggovidda	10	45	22	5
Smøla	18	150	12	8
Butendiek	33	288	11	9
Hollandse Kust	325	750	43	2
Meerwind	42	288	15	6

In Figure 8 we have tabulated gross area (km^2) and installed effect (MW) for some Norwegian onshore wind farms, and some European offshore farms. Our geographical grid is about 50×50 km in central Europe. With the density of the Smøla wind farm, this means 1 GW of installed capacity in a grid cell will occupy roughly 5% (gross) of the area.

Offshore density is smaller due to a larger wake effect; [1] suggests area use is 50% higher.

A.5 Consumption

We have downloaded hourly consumption data for the period 2006-2015 from ENTSO-E (publicly available), from Nordpool(subscription), and for Great Britain from National Grid ESO (`https://www.nationalgrideso.com/balancing-data/data-finder-and-explorer` *Historic demand Data*).

A.6 EMHIRES comparison

EMHIRES is an EU-project for providing capacity factors hour by hour, comparable to our data. The time series is based on MERRA-2, but onshore wind speeds are downscaled to each wind farm site in Europe by using wind speed Weibull densites from the Global Wind Atlas (GWA) ([5]). The assumption underlying the downscaling is that at any time, the MERRA wind and the site wind is at the same quantile in their respective distributions: Let F_m denote the cdf of the MERRA wind, and let F_s denote the cdf of the site wind from GWA. To find the wind speed v_s on site for a MERRA wind speed v_m, they solve the equation $F_s(v_s) = F_m(v_m)$ for v_s. In this way they are able to account for more local geographical features which affect the wind speed.

Figure 9 is a country level comparison between our capacity factors and the capacity factors from EMHIRES. For solar and offshore wind, our data aggregated to country level matches the EMHIRES data very well. For onshore wind, there are more deviations. For some countries, EMHIRES has a higher capacity factor, though for some countries (BE, DK, GB, LU and NL) it is the other way around. There can be many reasons for this. The EMHIRES data are based on actual wind farm locations with actual turbines, old and new, whereas our data are average over quite large areas with a fixed power curve. Typically, wind farms will be placed in locations where the wind is strong, and here the wind exceeds the average of the larger area.

Figure 9: Comparison with EMHIRES figures

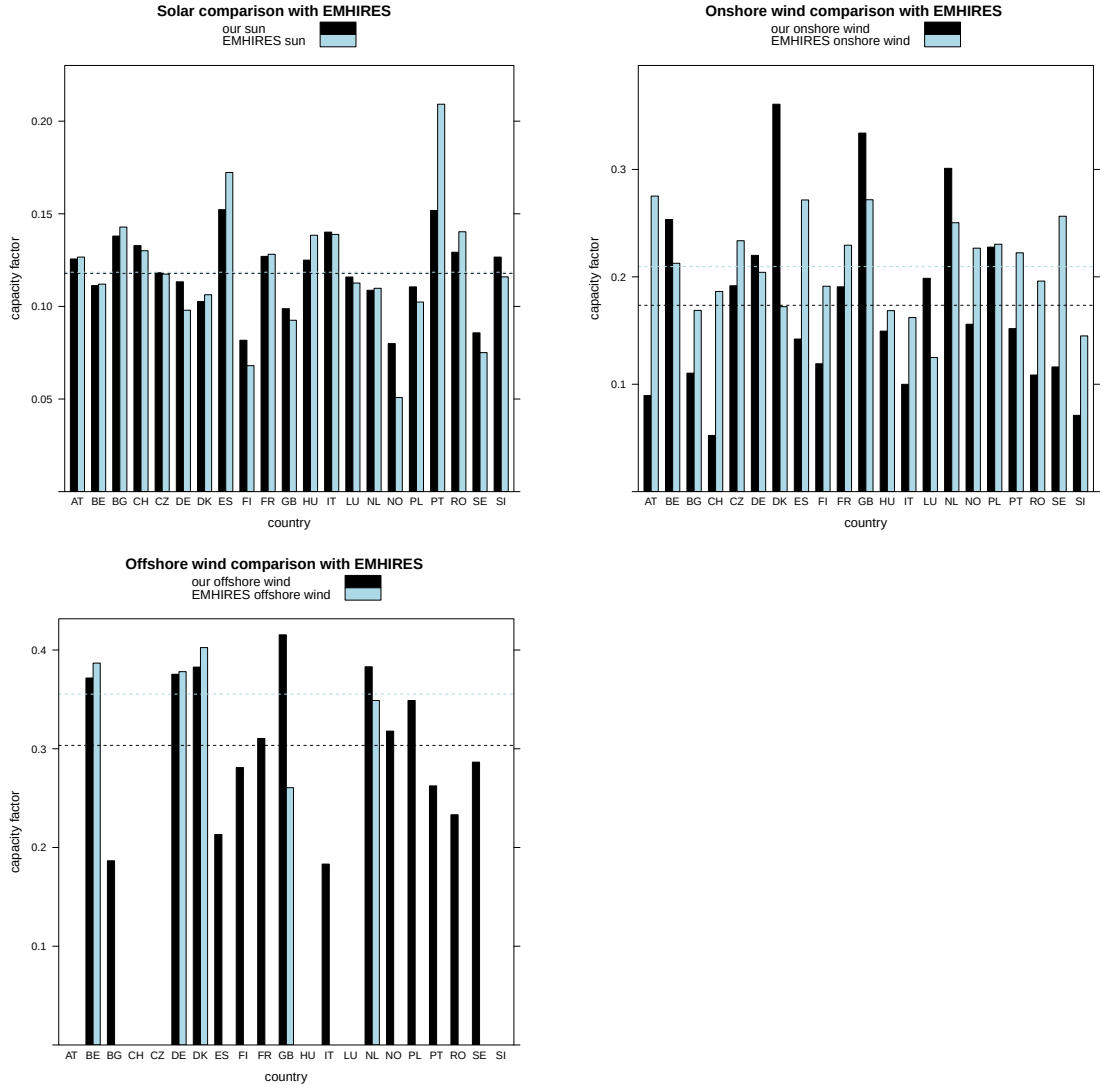

For small countries such as DK and BE, our classification of onshore/offshore can be inaccurate since many cells are both onshore and offshore.

A.7 References

[1] The European Wind Energy Association, *Europe's Energy Crisis. The No Fuel Solution*, February 2006.

[2] Francisco Bañuelos Ruedas, César Angeles-Camacho, and Sebastián Rios-Marcuello, *Methodologies Used in the Extrapolation of Wind Speed Data at Different Heights and Its Impact in the Wind Energy Resource Assessment in a Region*, Wind Farm - Technical Regulations, Potential Estimation and Siting Assessment (Gastón O. Suvire, ed.), InTech, Rijeka, 2011.

[3] John Boland, Barbara Ridley, and Bruce Brown, *Models of diffuse solar radiation*, Renewable Energy **33** (2008), no. 4, 575–584.

[4] Javier G. Corripio, *insol: Solar Radiation*, 2014, R package version 1.1.1.

[5] I. González-Aparicio, F. Monforti, P. Volker, A. Zucker, F. Careri, T. Huld, and J. Badger, *Simulating european wind power generation applying statistical downscaling to reanalysis data*, Applied Energy **199** (2017), 155 – 168.

[6] Fraunhofer IEE, *Full-load hours*, http://windmonitor.iee.fraunhofer.de/-windmonitor_en/3_Onshore/5_betriebsergebnisse/1_volllaststunden.

[7] Philippe Lauret, John Boland, and Barbara Ridley, *Bayesian statistical analysis applied to solar radiation modelling*, Renewable Energy **49** (2013), 124–127.

[8] J.F. Manwell, J.G. McGowan, and A.L. Rogers, *Wind Energy Explained: Theory, Design and Application*, 2 ed., Wiley, 2009.

[9] Edzer J. Pebesma and Roger S. Bivand, *Classes and methods for spatial data in R*, R News **5** (2005), no. 2, 9–13.

[10] REN21, *Renewables 2014. Global Status Report*, 2014.

[11] Andy South, *rworldxtra: Country boundaries at high resolution.*, 2012, R package version 1.01.

[12] Danijel Topić, Goran Knežević, and Krešimir Fekete, *The mathematical model for finding an optimal PV system configuration for the given installation area providing a maximal lifetime profit*, Solar Energy **144** (2017), 750–757.